PACS numbers: 85.60.Gz, 85.60.Bt; 81.07.–b; 42.25.Ja
DOI: 10.1070/QE2010v040n05ABEH014289

Effect of laser light polarisation on the dc photovoltage response of nanographite films

G.M. Mikheev, V.M. Styapshin, P.A. Obraztsov, E.A. Khestanova, S.V. Garnov

***Abstract*. We report an experimental study of the influence of pulsed 1064-nm laser light polarisation on the dc photovoltage response of nanographite films. The amplitude of the pulsed potential difference generated in the films across the plane of incidence is an even function of the angle between the plane of polarisation and the plane of incidence of the laser beam, and that along the plane of incidence is an odd function of this angle. We present empirical relations between the incident pulse power, parameters of elliptically polarised laser light and photovoltage amplitude. The results are interpreted in terms of surface electric currents due to the quasi-momentum transfer from the incident light to the electron system via interband quantum transitions and the surface photogalvanic effect.**

Keywords: *dc photovoltage response, photon drag, surface photoelectric emf, light polarisation, laser pulses, nanographite films.*

1. Introduction

The study of the mechanisms responsible for the dc photovoltage response of thin-film structures is of interest for the development of high-speed photodetectors and angle sensors. This effect manifests itself as a unipolar pulsed voltage (or emf) signal arising when a film is exposed to pulsed laser radiation. The pulsed emf response of Mo and W thin (50–270 nm) films exposed to laser pulses was attributed by Von Gutfeld [1] to an anisotropic Seebeck effect. The electric currents and the corresponding potential difference generated by high-power laser pulses in thin metallic (Ni, Ti, Bi) films grown on corrugated dielectric surfaces were accounted for by the formation of numerous in-plane regions with large temperature gradients (up to 10^7 K cm^{-1}), resulting in a Benedicks emf [2, 3]. Rather many reports have been concerned with a fast emf response of high-temperature superconductor films exposed to nanosecond laser pulses (see e.g. Refs [4–8]). According to Snarskii et al. [8], the key mechanism behind the dc photovoltage response of such films to laser pulses is the thermoelectric anisotropy of the films.

In previous works, the generation of nanosecond voltage pulses in porous nanographite films exposed to nanosecond laser pulses was interpreted in terms of optical rectification due to the quadrupole contribution to the second-order nonlinear susceptibility [9–12], as in the case of one-dimensional metallic photonic crystals [13]. At the same time, in systems with free carriers the pulsed voltage generated when laser light is obliquely incident on the surface to be studied can be understood in terms of photon drag, as in the case of bismuth films [14] and heterojunctions between two semiconductor structures [15]. The photon drag mechanism was used by Obraztsov et al. [16] to interpret the dc photovoltage response of mesoporous nanographite films and carbon nanotube yarns. A similar dependence of the pulsed photovoltage signal on the laser beam direction relative to the film surface, with a signal polarity reversal when the sign of the angle of incidence is changed, occurs when surface currents are due to the quasi-momentum transfer from the incident light to the electron system via interband quantum transitions [17] and in the case of the photogalvanic effect in thin films [18, 19]. The generation of surface currents in conductive materials has specific features pertaining to the dependence of the signal on incident light polarisation [19, 20]. In earlier studies of the photon drag effect in thin-film structures [14, 15] and the dc photovoltage response of porous nanographite films to nanosecond laser pulses [9–12], this dependence was not examined. This paper presents such data.

2. Experimental

In our experiments, we used nanographite films of dimensions 25×25 mm, produced by plasma-enhanced CVD from a methane-hydrogen mixture [21]. The substrates used were silicon wafers. The main structural components of films produced by this process are platelike crystallites composed of several (5 to 50) parallel, well-ordered graphene layers [22], preferentially oriented along the normal to the substrate surface. The thickness of the graphite nanocrystallites is 2 to 20 nm, and their lateral

G.M. Mikheev, V.M. Styapshin Institute of Applied Mechanics, Ural Branch, Russian Academy of Sciences, ul. T. Baramzinoi 34, 426067 Izhevsk, Russia; e-mail: mikheev@udman.ru;
P.A. Obraztsov A.M. Prokhorov General Physics Institute, Russian Academy of Sciences, ul. Vavilova 38, 119991 Moscow, Russia; present address: Department of Physics and Mathematics, University of Eastern Finland, Yliopistokatu 7, 80101 Joensuu Finland;
E.A. Khestanova Department of Physics, M.V. Lomonosov Moscow State University, Vorob'evy gory, 119991 Moscow, Russia;
S.V. Garnov A.M. Prokhorov General Physics Institute, Russian Academy of Sciences, ul. Vavilova 38, 119991 Moscow, Russia

Received 2 February 2010
Kvantovaya Elektronika **40** (5) 425–430 (2010)
Translated by O.M. Tsarev

dimensions (height, perpendicular to the substrate surface, and length, along the surface) are 1–3 μm.

The dc photovoltage response of the nanographite films was studied using 18-ns pulses of a passively Q-switched single-mode Nd^{3+} : YAG laser (*1*) (Fig. 1) [23]. The linearly polarised laser beam was passed through a quarter-wave plate (*3*) and directed to a Glan–Foucault prism (*4*), which served as a polariser. After a beam splitter (*5*), the beam was incident on the nanographite film (*6*) [on a silicon substrate (*7*)], which had parallel measuring electrodes DC (*8*) and AB (*9*) secured on its opposite sides. The electrodes were connected through a high-frequency cable to the input of a Tektronix TDS7704B 7-GHz digital oscilloscope (*10*). The ohmic resistance of the film between the electrodes was about 50 Ω. The plane of incidence of the beam contained the x axis of a rectangular system of coordinates, xyz, with the film surface in the xy plane, and the AB and CD electrodes were either normal (Fig. 1b) or parallel to the x axis (σ plane). Rotating the polariser around its axis, we were able to vary the angle Φ between the plane of the electric field vector, $\boldsymbol{E}$, and the plane of incidence, σ. Rotation of the nanographite film around the y axis allowed us to vary the angle of incidence of the beam, α. Angle Φ was measured clockwise from the laser beam direction.

In experiments with elliptically polarised light, polariser (*4*) was removed, and the laser beam was incident on the nanographite film surface at an angle $\alpha = 45^\circ$. The incident beam polarisation was successively converted from linear to elliptical, circular, elliptical and again linear. To this end, the quarter-wave plate was gradually rotated clockwise around its geometric axis relative to the laser beam direction, which caused the angle γ between its optical axis, lying in the plane of the plate, and the plane of polarisation of the incident beam to monotonically increase from 0 to 90°. The plane of the quarter-wave plate was normal to the laser beam. Thus, at $\gamma = 0$ and 90°, the beam emerging from the quarter-wave plate was linearly polarised, with the electric vector lying in the plane of incidence; at $\gamma = 45^\circ$, the beam was circularly polarised; in the range $0 < \gamma < 45^\circ$, the beam was elliptically polarised, with a polarisation azimuth angle $0 < \varphi < 45^\circ$; in the range $45^\circ < \gamma < 90^\circ$, the beam was elliptically polarised, with $-45^\circ < \varphi < 0$. Note that the polarisation azimuth, φ, characterises the orientation of the polarisation ellipse and is defined as the azimuth angle of the major axis of the ellipse.

The energy of laser pulses incident on the nanographite film, ε_{in}, was measured using the beamsplitter (*5*), which was nearly normal to the incident beam, and a calibrated photodetector (*11*), incorporated into a multichannel laser pulse detection system [24]. The neutral filters (*2*), (*12*) were used to reduce the beam power.

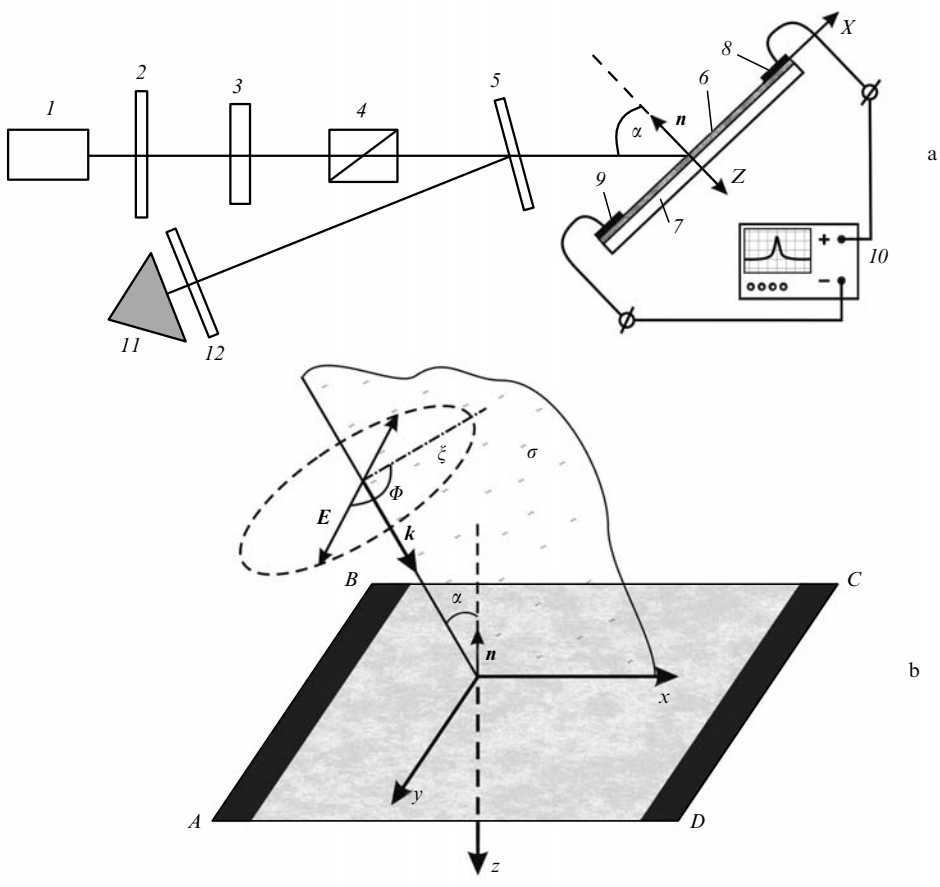

Figure 1. (a) Experimental arrangement and (b) schematic of the measuring electrodes AB and CD oriented perpendicular to the plane of incidence, σ, at oblique incidence of the beam on the film surface: (*1*) laser; (*2*, *12*) NS neutral optical filters; (*3*) quarter-wave plate; (*4*) polariser; (*5*) beamsplitter; (*6*) nanographite film; (*7*) substrate; (*8, 9*) measuring electrodes; (*10*) digital oscilloscope; (*11*) photodetector for measuring the laser pulse energy; xyz is a rectangular system of coordinates; $\boldsymbol{n}$ is the normal to the film surface; $\boldsymbol{k}$ is the wave vector of the incident beam ($\boldsymbol{k} \perp \xi$); and Φ is the angle between the plane of incidence, σ, and the plane of the electric field vector, $\boldsymbol{E}$.

3. Experimental results

First, the amplitudes U_x and U_y of the pulsed voltage between the parallel electrodes AB and CD oriented, respectively, perpendicular and parallel to the plane of incidence σ (to the x axis) were measured as functions of Φ at $\alpha = 45^\circ$. Because the signal amplitude is a linear function of ε_{in} [9, 10], we were able to obtain the conversion coefficients η_x and η_y as functions of Φ: $\eta_x(\Phi) = U_x\tau/\varepsilon_{\text{in}}$, $\eta_y(\Phi) = U_y\tau/\varepsilon_{\text{in}}$, where τ is the pulse duration. Figure 2 shows the measured η_x and η_y as functions of polarisation angle Φ. The $\eta_x(\Phi)$ data can be fitted by an even function [curve (*1*)] of the form

$$\eta_x = \eta_x^0(c_1 + \cos 2\Phi), \tag{1}$$

with $\eta_x^0 = 24.5$ mV MW^{-1} and $c_1 = 2.35$. The $\eta_y(\Phi)$ data are well fitted by an odd function [curve (*2*)] of the form

$$\eta_y = \eta_y^0 \sin 2\Phi. \tag{2}$$

with $\eta_y^0 = 43.7$ mV MW^{-1}.

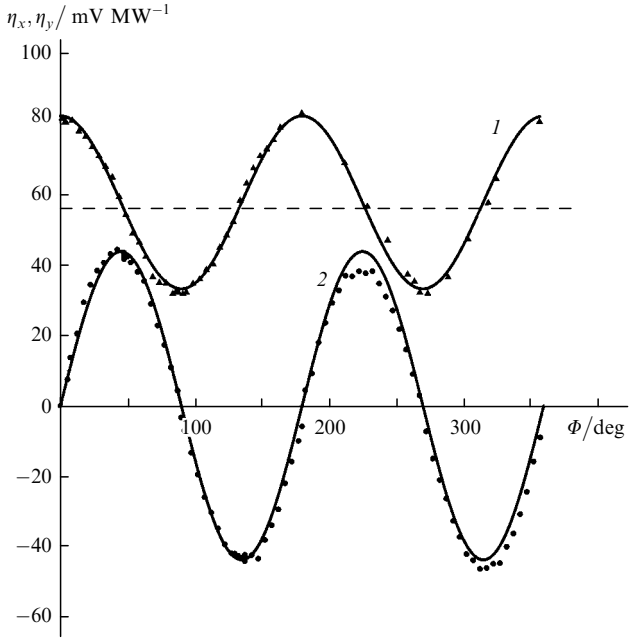

Figure 2. Measured optical power-to-voltage conversion coefficients, η_x and η_y, against the polarisation angle Φ of the linearly polarised incident beam for the measuring electrodes perpendicular (▲) and parallel (●) to the plane of incidence at an angle of incidence $\alpha = 45^\circ$; (*1*, *2*) fits to $\eta_x = \eta_x^0(c_1 + \cos 2\Phi)$ and $\eta_y = \eta_y^0 \sin 2\Phi$, respectively.

Therefore, the conversion coefficient η_x (at a constant angle of incidence $\alpha = 45^\circ$) is positive at any angle Φ between the plane of polarisation and the plane of incidence and has maxima at $\Phi = 0$ and 180° (p-polarisation) and minima at $\Phi = 90^\circ$, 270° (s-polarisation), in accordance with earlier results [9, 10]. The conversion coefficient η_y, obtained with the measuring electrodes parallel to the plane of incidence, has maxima in magnitude at $\Phi = 45^\circ$, 135°, 225°, 315°, and is positive at $\Phi = 45^\circ$ and 225° and negative at $\Phi = 135^\circ$ и 315°. At $\Phi = 0$, 180° (p-polarisation) and $\Phi = 90^\circ$, 270° (s-polarisation), η_y is zero, as already shown previously [9, 10].

Figure 3 shows the measured η_x as a function of the angle of incidence, α, at $\Phi = 0$, 45° and 90°, and the $\eta_y(\alpha)$ data at $\Phi = 45^\circ$. The conversion coefficients are seen to be odd functions of α. Of special note is that $\eta_x(\alpha)$ and $\eta_y(\alpha)$ differ markedly at $\Phi = 45^\circ$ and depend on the polarisation angle, Φ, as a parameter. A noteworthy feature of the $\eta_y(\alpha, \Phi = 45^\circ)$ curve is that it is well represented by a linear function in the range $-55^\circ < \alpha < 55^\circ$. Note also that, for a number of reasons, it is unfeasible to obtain reliable experimental data at angles of incidence close to ±90°. It is, however, obvious that η_x and η_y are zero at $\alpha = \pm 90^\circ$ because of the total reflection of the incident light.

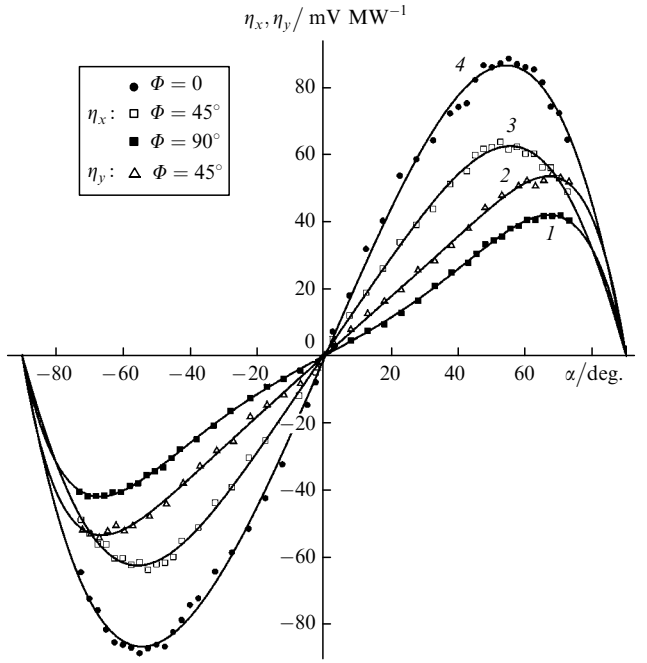

Figure 3. Measured η_x and η_y against the angle of incidence, α, at different polarisation angles, Φ, for the measuring electrodes perpendicular [$\eta_x - \Phi = 0$ (●), 45° (□), 90° (■)] and parallel [$\eta_y - \Phi = 45^\circ$ (△)] to the plane of incidence; (*1*–*4*) respective polynomial fits.

It follows from the experimental data in Figs 2 and 3 that the conversion coefficients η_x and η_y for linearly polarised laser radiation depend on the angle of incidence α and polarisation angle Φ as follows:

$$\eta_x = \eta_x^0 F_x(\alpha, \Phi)(c_1 + \cos 2\Phi), \tag{3}$$

$$\eta_y = \eta_y^0 F_y(\alpha, \Phi) \sin 2\Phi, \tag{4}$$

where $F_x(\alpha, \Phi)$ and $F_y(\alpha, \Phi)$ are odd functions of α, with zeros at $\alpha = 0$ and ±90°, and depend little on Φ.

The experimental data in Fig. 4 illustrates the influence of angle γ, which determines the degree of ellipticity, on the conversion coefficients η_x and η_y at an angle of incidence $\alpha = 45^\circ$. It follows from Fig. 4 that the $\eta_x(\gamma)$ and $\eta_y(\gamma)$ data can be fitted by functions of the form

$$\eta_x = \eta_x^{0\gamma}(c_2 + \cos 4\gamma), \tag{5}$$

$$\eta_y = \eta_y^{0\gamma} \sin 4\gamma, \tag{6}$$

with $\eta_x^{0\gamma} = 14.5$ mV MW^{-1}, $\eta_y^{0\gamma} = 24$ mV MW^{-1} and $c_2 = 4.7$. The η_y coefficient has zeros at $\gamma = 0$, 45° and 90°. That the conversion coefficient η_y is zero at $\gamma = 0$ and 90°, when p-polarised laser radiation ($\Phi = 0$) traverses the quarter-wave plate with no changes in polarisation, correlates with the results represented by curve (*2*) in Fig. 2. At $\gamma = 45°$, the beam emerging from the quarter-wave plate is circularly polarised, and its interaction with the nanographite film produces no dc photovoltage response. The shape of the experimental $\eta_y(\gamma)$ curve indicates that the signal polarity for elliptically polarised light is independent of the electric field vector rotation direction and is determined by the polarisation azimuth, φ.

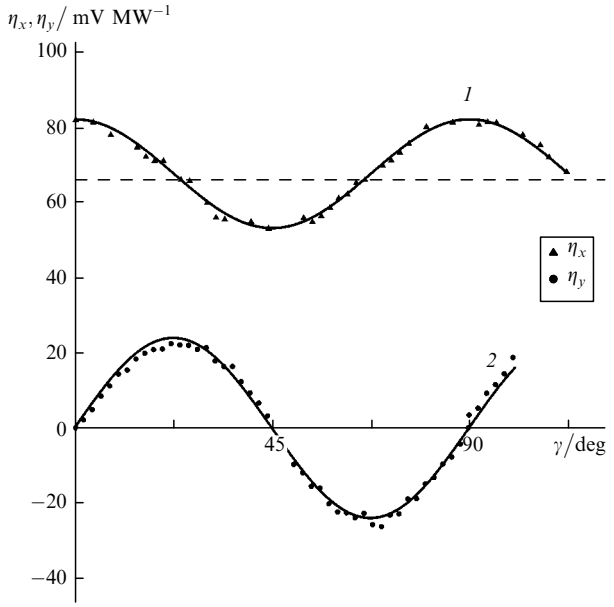

Figure 4. Measured η_x and η_y against γ (the angle between the optical axis of the quarter-wave plate and the plane of polarisation of p-polarised radiation) for the measuring electrodes perpendicular (η_x, ▲) and parallel (η_y, ●) to the plane of incidence at an angle of incidence $\alpha = 45°$; (*1, 2*) fits to $\eta_x = \eta_x^{0\gamma}(c_2 + \cos 4\gamma)$ and $\eta_y = \eta_y^{0\gamma} \sin 4\gamma$, respectively.

Thus, when the measuring electrodes are parallel to the plane of incidence, p-, s- or circularly polarised laser light induces no photovoltage signal. Note that, as demonstrated by curve (*1*) in Fig. 4, the conversion coefficient η_x, obtained with the measuring electrodes perpendicular to the plane of incidence, has a minimum for circularly polarised laser light.

4. Discussion

The above experimental data can be interpreted in terms of the electric current due to the surface photogalvanic effect and the quasi-momentum transfer from the incident light to the electron system via interband quantum transitions. According to Al'perovich et al. [19], light incident obliquely on an isotropic crystal may induce a surface-parallel electric current due to the photogalvanic effect. Such a current was detected by them in GaAs epitaxial layers at $T = 1.6$ and 4.2 K and was attributed to the fact that the bulk and surface of the crystal differed in the momentum relaxation rates for electrons and holes involved in interband optical transitions. Assuming that $n^2 \gg 1$ (where n is the index of refraction) and using Frenkel formulas for linearly polarised light, Al'perovich et al. [19] derived expressions for the surface current densities J_x and J_y in the directions lying in the plane of incidence and in a plane normal to the plane of incidence, respectively, as functions of angles α and Φ:

$$J_x = aI \frac{\sin 2\alpha \cos\alpha (1 + \cos 2\Phi)}{2(n\cos\alpha + 1)^2}, \tag{7}$$

$$J_y = aI \frac{\sin 2\alpha \cos\alpha \sin 2\Phi}{4(n\cos\alpha + 1)(n + \cos\alpha)}, \tag{8}$$

where a is a frequency-dependent scalar function and I is the incident light intensity.

According to Gurevich and Laiho [20], the photomagnetism detected in a polycrystalline copper plate ($T = 4.2$ K) exposed to an obliquely incident linearly polarised laser beam may be due to the surface currents resulting from the photogalvanic effect and the quasi-momentum transfer from the incident light to electrons via interband quantum transitions. The following expressions were derived for the surface current densities J_x and J_y due to the photogalvanic effect:

$$J_x = \frac{b}{2}|E_0|^2 \mathrm{Re}(\varepsilon^{-1}) \sin 2\alpha (1 + \cos 2\Phi), \tag{9}$$

$$J_y = \frac{b}{2}|E_0|^2 \mathrm{Re}(\varepsilon^{-1}) \sin\alpha \sin 2\Phi, \tag{10}$$

where b depends on the electronic spectrum and incident light frequency; E_0 is the electric field amplitude; and ε is the complex dielectric permittivity. In addition, Gurevich and Laiho [20] presented expressions for the surface current densities J_x and J_y due to the quasi-momentum transfer from the incident light to electrons via interband quantum transitions:

$$J_x \propto (\mathrm{const} + \cos 2\Phi), \tag{11}$$

$$J_x \propto \sin 2\Phi. \tag{12}$$

These relations were obtained in the simplest model of the electronic spectrum [17], for $l \gg \delta$ and $|\varepsilon| \gg 1$, where l is the electron mean free path and δ is the penetration depth of the light in the material.

In comparing the present experimental data to the above relations, it should be noted first of all that the multipliers in relations (7)–(10) for $J_x(\alpha)$ and $J_y(\alpha)$ were obtained theoretically without allowance for the reflectivity of the surface [20] or with allowance for the Fresnel formulas for $n^2 \gg 1$ [19]. These approximations are invalid for the absorbing nanographite film studied here. At the same time, the multipliers in relations (8), (10) and (12) for J_y, which represent the theoretical signal amplitude as a function of

polarisation angle, Φ, coincide with the experimentally determined one in Eqn (4). Relation (12) applies to both the surface photogalvanic effect and the surface current arising from the quasi-momentum transfer from the incident light to the electron system via interband quantum transitions. The experimentally determined multiplier in (3), which describes the influence of the polarisation angle, Φ, on the dc photovoltage response when the measuring electrodes are perpendicular to the plane of incidence, coincides with the multiplier in (11), derived theoretically by Gurevich and Laiho [20]. Note that, according to (7) and (9), the $J_x(\Phi)$ dependence for the surface photogalvanic effect is a particular case of relation (11), derived for the surface current due to the quasi-momentum transfer from the incident light to electrons [20]. Thus, the experimentally determined $\eta_x(\Phi)$ and $\eta_y(\Phi)$ dependences for linearly polarised laser light in (3) and (4) coincide with the theoretical dependences (11) and (12), respectively.

As shown in our additional experiments, relations (3) and (4) are also valid for silver- and palladium-based resistive films, which exhibit a similar dc photovoltage response [25]. It is quite probable that relations similar to (3) and (4) might be obtained by repeating experiments with bismuth films [14] and heterojunctions between two semiconductor structures [15].

To our knowledge, the effects under discussion, resulting in surface currents, have not been considered for an arbitrary elliptical polarisation of light. Using the experimental data in Fig. 4 and Eqns (3) and (4), we can find the conversion coefficients η_x and η_y for elliptically polarised light. At a given angle of incidence, α, we have

$$\eta_x = \eta_x^{0\alpha}\left(c_2 + \frac{a^2 - b^2}{a^2 + b^2}\right)\cos 2\varphi, \tag{13}$$

$$\eta_y = \eta_y^{0\alpha}\frac{a^2 - b^2}{a^2 + b^2}\sin 2\varphi, \tag{14}$$

where $\eta_x^{0\alpha}$, $\eta_y^{0\alpha}$ are the conversion coefficients dependent on the angle of incidence, α; a and b are the major and minor axes of the polarisation ellipse; and φ is the azimuth angle of the major axis of the polarisation ellipse. As shown in additional experiments with elliptical polarisation obtained at various angles Φ of linearly polarised light incident on the quarter-wave plate, the experimental data are well represented by Eqns (13) and (14).

It should further be noted that the generation of U_x and U_y pulsed voltages between the measuring electrodes AB and CD oriented, respectively, perpendicular and parallel to the plane of incidence, σ, points to the development of ring currents on the film surface under open-circuit conditions, that is, when the electrodes are not connected into an electrical circuit. According to the experimental data presented in Figs 2 and 3, such currents may flow both clockwise and anticlockwise, depending on the polarisation angle, Φ, and are zero when the incident laser light is p-, s- or circularly polarised.

5. Conclusions

Measurements of the dc photovoltage response of nanographite films to 1064-nm laser pulses show that, when the measuring electrodes are parallel to the plane of incidence, the signal amplitude varies as the sine of double the polarisation angle, Φ, with zeros at $\Phi = 0$ (p-polarisation) and $\Phi = 90^\circ$ (s-polarisation) and a maximum at $\Phi = 45^\circ$. When the measuring electrodes are normal to the plane of incidence, the signal amplitude comprises a constant component, independent of the polarisation angle, and a component that varies as $\cos 2\Phi$. At a given angle of incidence, the signal polarity is independent of Φ, and the signal amplitude has a maximum and minimum for p- and s-polarised light, respectively. When the incident laser light is elliptically polarised, the signal depends significantly on the degree of ellipticity, polarisation azimuth and the orientation of the measuring electrodes relative to the plane of incidence. With the measuring electrodes parallel to the plane of incidence and a circular polarisation, there is no signal. When the incident laser light is linearly polarised with a polarisation angle $\Phi = 45^\circ$, the variation of the signal amplitude with the angle of incidence, α, strongly depends on whether the measuring electrodes are parallel or perpendicular to the plane of incidence. The present experimental data can be understood in terms of the surface photogalvanic effect and the quasi-momentum transfer from the absorbed light to the electron system.

Acknowledgements. We are grateful to T.N. Mogileva for her useful comments and assistance in the experimental work. We thank A.N. Obraztsov and Yu.P. Svirko for valuable discussions. This work was supported by the Russian Foundation for Basic Research (Grant Nos 08-02-91755 and 10-02-96017-r_ural) and the Academy of Finland (Project Nos 123252 and 133359).

References

1. Von Gutfeld R.J. *Appl. Phys. Lett.*, **23**, 206 (1973).
2. Konov V.I., Nikitin P.I., Satyukov D.G., Uglov S.A. *Izv. Akad. Nauk SSR. Ser. Fiz.*, **55**, 1343 (1991).
3. Grigorenko A.N., Nikitin P.I., Jelski D.A., George T.F. *J. Appl. Phys.*, **69**, 3375 (1991).
4. Chang C.L., Kleinhammers A., Moultan W.G., Testardi L.R. *Phys. Rev. B*, **41**, 11564 (1990).
5. Nikishin V.A., Sevenyuk A.A., Sukhov A.V. *Kvantovaya Elektron.*, **18**, 1103 (1991) [*Sov. J. Quantum Electron.*, **21**, 999 (1991)].
6. Kwok H. S., Zheng J.P. *Phys. Rev. B*, **50**, 14561 (1994).
7. Zeuner S., Prettl W., Lengfellner H. *Appl. Phys. Lett.*, **66**, 1833 (1995).
8. Snarskii A.A., Pal'ti A.M., Ashcheulov A.A. *Fiz. Tekh. Poluprovodn.*, **31**, 1281 (1997).
9. Mikheev G.M., Zonov R.G., Obraztsov A.N., Svirko Yu.P. *Appl. Phys. Lett.*, **84**, 4854 (2004).
10. Mikheev G.M., Zonov R.G., Obraztsov A.N., Svirko Yu.P. *Zh. Eksp. Teor. Fiz.*, **126**, 1083 (2004).
11. Mikheev G.M., Zonov R.G., Obraztsov A.N., et al. *Pis'ma Zh. Tekh. Fiz.*, **31** (3), 11 (2005).
12. Mikheev G.M., Zonov R.G., Obraztsov A.N., et al. *Prib. Tekh. Eksp.*, **3**, 84 (2005).
13. Hatano T., Nishikawa B., Iwanaga M., Ishihara T. *Opt. Express*, **16**, 8236 (2008).
14. Beregulin E.V., Valov P.M., Ryvkin S.M., et al. *Pis'ma Zh. Eksp. Teor. Fiz.*, **25**, 113 (1977).
15. Beregulin E.V., Voronov P.M., Ivanov S.V., et al. *Pis'ma Zh. Eksp. Teor. Fiz.*, **59**, 83 (1994).
16. Obraztsov A.N., Lyashenko D.A., Fang S., et al. *Appl. Phys. Lett.,* **94**, 231112 (2009).

17. Gurevich V.L., Laiho R. *Phys. Rev. B*, **48**, 8307 (1993).
18. Magarill L.I., Entin M.V. *Fiz. Tverd. Tela*, **21**, 1280 (1979).
19. Al'perovich V.L., Belinicher V.I., Novikov V.N., Terekhov A.S. *Zh. Eksp. Teor. Fiz.*, **80**, 2298 (1981).
20. Gurevich V.L., Laiho R. *Phys. Sol. State*, **42,** 1807 (2000).
21. Zolotukhin A.A., Obraztsov A.N., Ustinov A.O., Volkov A.P. *Zh. Eksp. Teor. Fiz.*, **124**, 1291 (2003).
22. Obraztsov A.N., Pavlovskii I.Yu., Volkov A.P. *Zh. Tekh. Fiz.*, **71**, 89 (2001).
23. Mikheev G.M., Maleev D.I., Mogileva T.N. *Kvantovaya Elektron.*, **19**, 45 (1992) [*Quantum. Electron.*, **22**, 37 (1992)].
24. Mikheev G.M., Mogileva T.N., Popov A.Yu., et al. *Prib. Tekh. Eksp.*, **2**, 101 (2003).
25. Mikheev G.M., Zonov R.G., Aleksandrov V.A., et al. RF Patent No. 2365027, 20.08.09.